Proceedings of the 16th International Conference on Soil Mechanics and Geotechnical Engineering

doi:10.3233/978-1-61499-656-9-939

Use of DEM to analyse incremental strains along localizations in granular materials

L'emploi des méthodes aux eléments discrets pour analyser les déformations incrémentielles le long des localisations dans les matériaux grenus

Catherine O'Sullivan
Imperial College London
Jonathan D. Bray
University of California, Berkeley

ABSTRACT

Developing an understanding of the relationship between dilation along shear bands and shear strength of soil has been the focus of much research in soil mechanics. While significant insight has been achieved using photographic techniques and X-ray methods, the accuracy and resolution of these measurements are limited. Discrete element methods are convenient tools to analyse the evolution of localizations in granular materials in some detail. The current paper describes the use of the distinct element method to quantify the incremental volumetric and shear strains along localizations in dense granular materials during compression tests. For idealized granular materials comprising uniform disks or spheres in regular packing arrangements, the incremental strains are relatively uniform along the shear band. There is also a clear correlation between the incremental volumetric strains along the localization and the macro-scale response. For irregular, non-uniform specimens this correlation is less clear and the incremental strains along the localization are highly non-uniform, with both contraction and dilation being observed within the zone of localization during a single increment of axial strain.

RÉSUMÉ

Comprendre la relation entre la dilation le long des bandes de cisaillement et la résistance au cisaillement des sols a fait l'objet de nombreuses recherches en mécanique des sols. Les techniques photographiques et les méthodes utilisant les rayons X ont permis des progrès significatifs dans ce domaine, mais restent limitées du point de la résolution et de la précision. Les méthodes aux éléments discrets constituent un outil commode pour analyser plus en détail l'évolution des localisations dans les matériaux grenus. Le présent article décrit l'utilisation des éléments distincts pour quantifier la déformation en cisaillement incrémentielle le long de localisations dans les sols grenus denses lors d'essais en compression. Pour des matériaux grenus idéaux constitués de disques uniformes ou de sphères en assemblages réguliers, les déformations incrémentielles sont relativement uniformes le long de la bande de cisaillement. Une corrélation entre les déformations volumiques incrémentielles le long des localisations et la réponse à l'échelle macroscopique peut clairement être observée. Pour des spéciments irréguliers et non-uniformes, cette corrélation est moins claire et les déformations incrémentielles le long de la localisatio sont extrêmement hétérogènes, puis qu'on peut observer à la fois le phénomène de contraction et celui de dilation au niveau de la zone de localization pendant un incrément de défomation axiale.

1 INTRODUCTION

As noted by Bolton (1986) much of the early research exploring the relationship between strength and dilatancy of sand used strain values calculated based on the displacement of the specimen boundaries and the measured overall volume changes and underestimated the dilatancy. While further insight has been gained through X-ray methods (e.g. Oda and Kazama (1998)) and photographic analysis (e.g. Gudehus and Nubel (2004)), such methods are limited in their resolution and accuracy. In a discrete element analysis, the displacements of each particle can be monitored throughout the simulation. Consequently accurate measurements of local strain can easily be made.

The current study examines the results of some discrete element simulations to explore the relationship between dilation and specimen response in dense granular materials. The paper firstly gives a brief overview of the discrete element simulations as well as approach used to calculate the local strain values. Three series of simulations are then discussed. The first series of simulations considers two-dimensional biaxial compression tests on disks with a hexagonal packing, the second series of simulations considers plane strain compression tests on three dimensional specimens of uniform spheres, and the final series of simulations considers biaxial compression tests on dense polydisperse specimens of disks.

2 ANALYTICAL APPROACH

2.1 *Discrete Element Simulations*

The two-dimensional analyses presented here comprise simulations of strain controlled biaxial compression tests using the distinct element method (DEM) software PFC^{2D} (Itasca, 2002). In these simulations the cell pressure is applied using the virtual stress controlled membrane algorithm proposed by Thomas (1997). The advantage of using a membrane is that localizations can more easily develop in the material. Contact was modeled using linear normal and shear penalty springs.

The three-dimensional plane strain simulations used the three-dimensional DEM code, 3D-DEM, described by O'Sullivan (2002). As with the two-dimensional simulations contact was modeled using linear springs and a three-dimensional stress controlled membrane was used.

2.2 *Non-Linear Kinematic Homogenization*

The DEM simulations give the particle displacements and rotations during the test simulation; an additional set of calculations are then required to calculate the local strain values. O'Sullivan et al (2003) proposed a method for kinematic homogenization that is capable of capturing particle rotation and that uses non-linear interpolation. In this homogenization method the effects of rotation are included by tracking the displacement of two points on each particle, instead of considering only the displacement of the particle centroids

(Figure 1(a)). A rectangular grid is generated to serve as a referential continuum discretization over the volume of particles under consideration Figure 1(b). The interpolated displacements and displacement gradients are then calculated at these grid points using the cubic wavelet functions illustrated in Figure 1(c). The radius of the wavelet function is the area over which each particle contributes to the interpolated displacement field, and hence the average strain field. For the analyses discussed here the wavelet radius is a multiple of the particle radius. Note that the strain values were calculated using large strain theory.

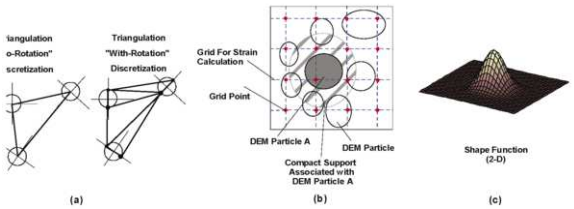

Figure 1: Illustration of homogenization approach used (a) Angle of mobilized friction versus axial strain, (b) Specimen coordination number versus axial strain.

3 REGULAR SPECIMENS – 2D

Idealized granular materials, i.e. rods in two-dimensions and balls in three-dimensions, have been used as analogue soils in a number of studies including Rowe (1962). The response of hexagonally packed disks in biaxial compression and the sensitivity of the response to small changes in the disk geometry was considered in some detail by O'Sullivan et al (2002) who coupled DEM simulations and accurate physical tests. This earlier study highlighted the importance of coordination number along with its sensitivity to particle geometry. The current study directly extends this earlier work to analyse in detail the relationship between dilation along the shear band in a test specimen and the macro-specimen response.

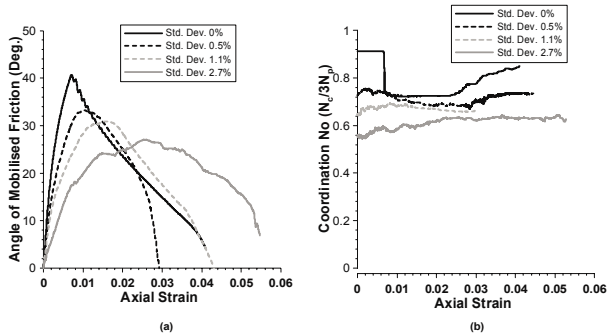

Figure 2: Response of hexagonally packed disk specimens (a) Angle of mobilized friction versus axial strain, (b) Specimen coordination number versus axial strain.

The simulations comprised biaxial compression tests on 5.8 mm perfectly round disks (158 each), in which the standard deviation of the rod radii was systematically varied. A contact spring stiffness of 5 x 10^7 N/m was used for these simulations, the particle density was assumed to 7.85 x 10^7 kg/m3 and a mean inter-particle friction angle of 12.1^o was assumed (O'Sullivan et al 2002). The peak strength of this assembly is sensitive to minor variations in the distribution of disk radii. Increasing the standard deviation from 0.5% to 2.7% caused both the peak strength to decrease and the specimen stiffness to decrease. (Figure 2 (a)). O'Sullivan et al (2002) related the chances in response to a decrease in the average coordination number (Figure 2 (b)) as the size distribution of the disks increased.

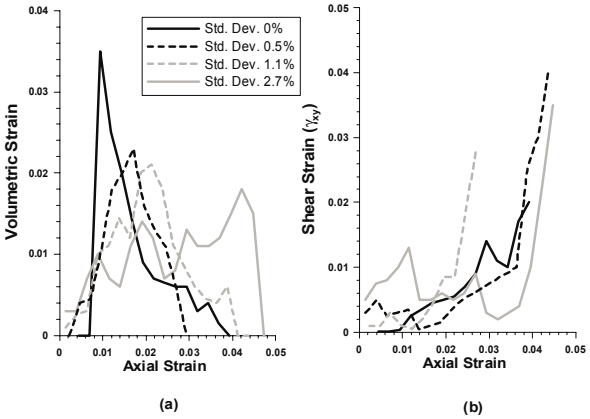

Figure 3: Local incremental strains for hexagonally packed specimens (a) Incremental volumetric strain along localization versus axial strain (b) Incremental shear strain along localization (γ_{xy}) versus axial strain.

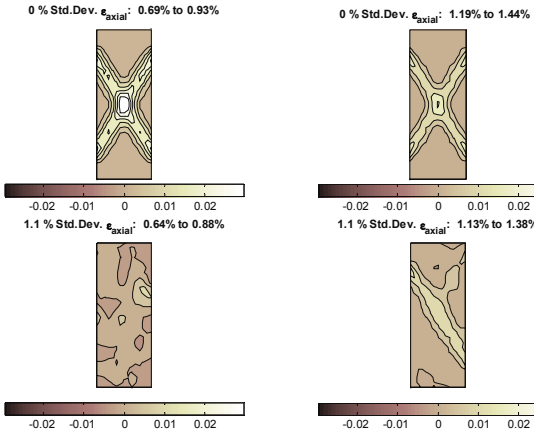

Figure 4: Comparison of incremental volumetric strain values for the uniform specimen (0% Std. Dev.) and the specimen at with 1.1% standard deviation in disk sizes for corresponding axial strain increments.

In the current analysis, the incremental volumetric ε_{vol} and shear strains γ_{xy} along the localization were calculated for axial stain increments of 0.25% using the homogenization approach described above. Figure 3 illustrates the variation of the local strain values as a function of axial strain (ε_{axial}) for the tests considered in Figure 2. There is a clear correlation between the results presented in Figure 2(a) and Figures 3(a). The peak incremental volumetric strains (i.e. dilation) are observed at axial strains close to the axial strains where the peak stresses are mobilized. Furthermore, there is a systematic decrease in the maximum volumetric strain increments along the localization with increasing distribution of the particle sizes.

The incremental volumetric strains for two corresponding increments of axial strain for the uniform disk specimen and the specimen with a disk size standard deviation of 1.1% are illustrated in Figure 4. The axial strain increment 0.69% to 0.93% corresponds to the increment with the maximum dilation for the uniform specimen, while the axial strain increment 1.13% to 138% corresponds to the increment with the maximum dilation for the uniform specimen for the specimen with a standard deviation of 1.1%. For both specimens the incremental volumetric strains along the localizations at their peak values are relatively uniform and are a maximum towards the center of the localization. Two conjugate and equivalent localizations are observed in the uniform specimen as a consequence of the perfect symmetry of the specimen. The maximum volumetric strains for the specimen with a standard

deviation of 1.1% are clearly smaller than those obtained for the uniform specimen, in line with the results presented in Figure 3.

Considering the shear strain values (Figure 3(b)), the incremental shear strain values are close to their minimum values at the point of maximum dilation (i.e. maximum incremental volumetric strain). Furthermore, the incremental shear strains continue to increase with increasing axial strains after the peak stress has been mobilized, while the incremental volumetric strains are progressively decreasing.

4 REGULAR SPECIMENS – 3D

In three dimensions, for uniform-sized spheres, both the face-centered-cubic (FCC) packing and the rhombic (or hexagonal-close) packing give the maximum packing density. An earlier study considered response of both these packing configurations using physical tests coupled with DEM simulations (O'Sullivan et al (2004)). The results of simulations of plane strain tests on uniform-sized ball specimens with both FCC and rhombic packings are illustrated in Figures 5 (a). The spheres used in both simulations had average inter-particle friction angles of 5.71^o. The response is similar to the response of the hexagonally packed disks discussed above. Initially, the response is very stiff until the peak strength is mobilized. The subsequent post-peak drop in deviatoric stress is relatively rapid and monotonic. The differences in strength as a function of packing are clearly seen here, with FCC-packed specimen yielding a peak angle of mobilized friction value of 24.2^o and rhombic-packed specimen test yielding a peak friction angle of 40.5^o. O'Sullivan et al (2004) related these differences in strength to differences in the fourth order fabric tensor, F_{iiii}.

Figure 5(b) illustrates the variation in the incremental volumetric strains for these two test simulations for axial strain increments of 0.4%. The relationship between the incremental volumetric strains and the macro-scale response (i.e. angle of mobilized friction) is similar to the trend observed for the two-dimensional biaxial compression tests on hexagonally packed disks described above. The maximum dilation is observed close to the axial strain where the peak stress is mobilized. Furthermore there is a relationship between the specimen strength and the incremental volumetric strain, with the rhombic specimens exhibiting higher peak incremental volumetric strain values in comparison with the FCC specimen. Whereas the incremental shear strains increase post peak, the increase is not as marked as for the two-dimensional tests. The incremental shear strains are similar for both specimens at corresponding axial strains values.

5 RANDOM SPECIMENS

The first two series of simulations considered the idealized case of specimens of uniform or almost uniform particles with regular packing configurations. Real soils have irregular packing configurations and a wide distribution of particle sizes. As a first attempt to extrapolate these results to soil, two discrete element simulations of dense biaxial compression tests on randomly arranged disks were performed. The two specimens considered were equivalent, but had different numbers of particles, so that scaling effects could be examined. Specimen A contains 5,728 disks (Figure 6(b)) and "Specimen B" contains 12,512 disks. Both specimens were created using the specimen generation approaches proposed by Itasca (2002); the particle radii were generated to be uniformly distributed between 0.075 cm and 0.100 cm and to have an initial porosity of 0.1. Specimen A had dimensions 9 cm by 18 cm while Specimen B had dimensions 18 cm by 36 cm. For both simulations the particle density was 20 $x10^9$ kg / m^3, the spring stiffnesses were 5 x 10^7 N/m, the damping parameter (PFC damping) was 0.20, and the inter-particle coefficient of friction was 0.3. Note that in contrast to the simulations discussed above these simulations do not relate to a series of physical tests.

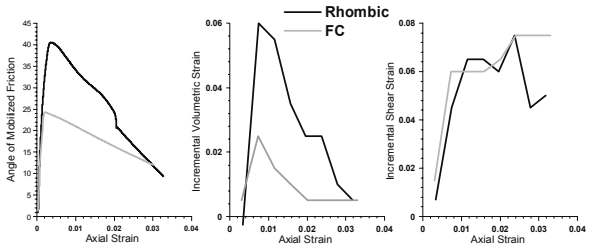

Figure 5: Comparison response of rhombic and face-centered-cubic packed specimens of uniform spheres in plane strain compression: (a) Angle of mobilized friction versus axial strain, (b) Incremental volumetric strains versus axial strain, (c) Incremental shear strains versus axial strain.

For both specimens, the angle of friction mobilized as a function of axial strain is illustrated in Figure 6(a). The response for both specimens is equivalent; the smaller specimen ("Specimen A", 5,728 disks) attained a peak angle of mobilized friction of 22.0^o at an axial strain of 1.3%, while the larger specimen ("Specimen B", 12,512 disks) attained a peak angle of mobilized friction of 21.7^o at an axial strain of 1.2%. O'Sullivan (2002) noted that an examination of plots of the incremental displacements for "Specimen A" and "Specimen B" indicated that the deformation pattern for both specimens is similar; at small strain levels the displacement localizations are not distinguishable, however with increasing strain two localization areas can clearly be seen. O'Sullivan (2002) also included an analysis of the particle rotations in each specimen and demonstrated quantitatively that despite the differences in particle size, the particle rotation values were equivalent for both simulations

The analysis of local strain values for these two simulations firstly considered the selection of homogenization parameters so that the calculated local strain values would be equivalent. For both specimens incremental volumetric and shear strains were calculated for axial strain increments of 0.5%. For Specimen A the wavelet radius used in the non-linear interpolation was 4 times the particle radius (Figure 1(c)) and a grid of 40 points by 80 points was used (Figure 1(b)). For the larger specimen (Specimen B) two analyses were carried out. In the first case the wavelet radius was 4 times the particle radius and a grid of 80 points by 160 points was used so that the ratio of the grid spacing to the particle radius was the same as for the analysis of "Specimen A". In the second analysis, the wavelet radius was 8 times the particle radius and a grid of 40 points by 80 points was used so that the ratio of the grid spacing to the specimen width was the same as for the analysis of "Specimen A". Figure 7(a) illustrates the maximum positive incremental volumetric strain versus the axial strain for the analyses, while Figure 7(b) illustrates the maximum incremental shear strain (γ_{xy}) for these analyses as a function of axial strain. As illustrated in Figure 7, when the ratio of the wavelet radius to the specimen width and the ratio of the grid spacing to the specimen width are consistent, the calculated strain values are equivalent. However, higher values of localized volumetric strain are calculated in the shear band when a small window is used, indicating that in zones where the strain is highly variable, the calculated strain is sensitive to the size of the window selected.

Considering the results presented in Figure 7, the correlation between the maximum dilation and the macro-scale response is less distinct than for the uniform specimens. While there is an increase in the observed dilation up until the peak strength is mobilized, the post peak decrease in dilation observed in Figures 3 and 5 is not evident. This is because the response along the localization is no longer uniform. Figure 8 illustrates

the incremental volumetric strains for both specimens close to the point where the peak stress is mobilized. For both specimens both the principle and conjugate localizations are evident. At this point both dilation (positive incremental strains) and contraction (negative incremental strains) are evident along the localization. This variation in strains becomes more apparent post-peak and can most likely be related to the formation and collapse of load bearing columns of particles in the specimen Oda and Kazama (1998). Future analysis will consider the local forces and stresses in more detail.

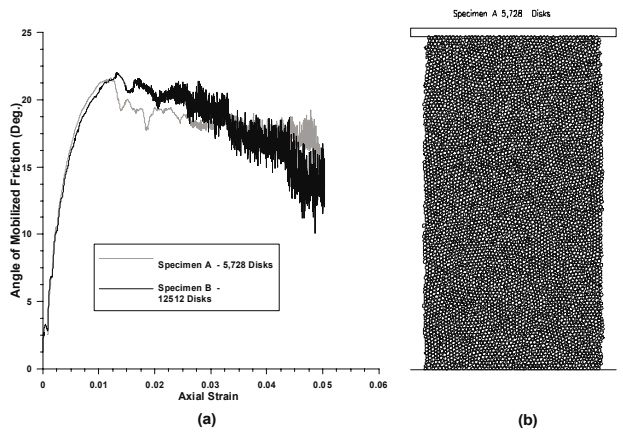

Figure 6: (a) Angle of mobilized friction versus axial strain for dense random two-dimensional specimens in biaxial compression (b) Illustration of Specimen A (5728 disks).

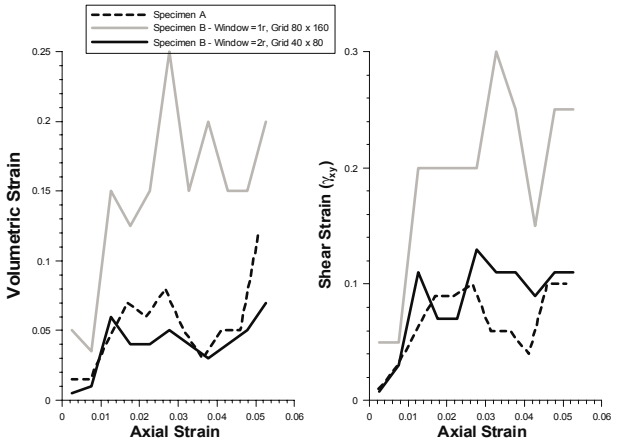

Figure 7: Incremental strains for dense two-dimensional specimens (a) Incremental volumetric strain versus axial strain (b) Incremental shear strain versus axial strain.

6 SUMMARY

This paper describes the use of DEM analyses to explore in detail the relationship between the incremental volumetric and shear strains along localizations and the macro-scale response of granular materials. For the idealized cases of uniform and almost uniform specimens of disks and spheres with regular packing configurations, there is a clear correlation between the incremental volumetric strains and the macro-scale specimen response. Furthermore, the distribution of incremental strains along the localization is relatively uniform for these idealized configurations. For dense random two-dimensional specimens of disks subject to biaxial compression, the distribution of strains along the localization was non-uniform, with incremental dilation and incremental contractions being observed at different locations along the shear band in the same increment of axial strain. The correlation between the macro-scale response and the maximum positive incremental volumetric strain is less clear than for the case of uniform, regular specimens. When a non-local interpolation approach is used to calculate the local strain values, the calculated strains will be scale-independent provided the ratio of the size of the wavelet interpolant to the problem domain and the ratio of the grid spacing to the problem domain remains constant.

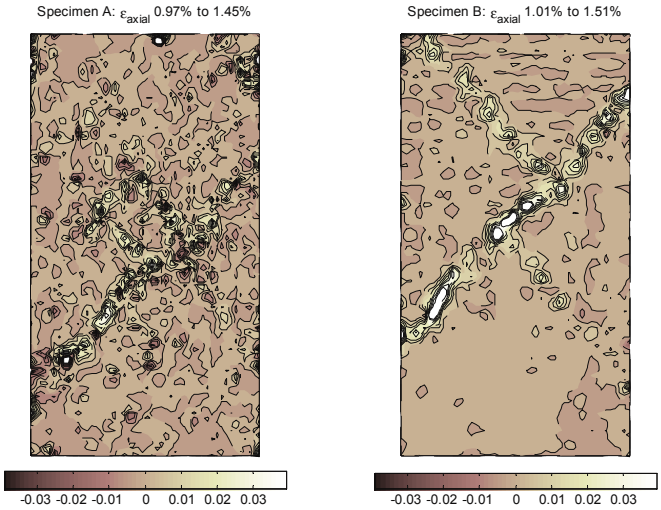

Figure 8: Contours of incremental volumetric strains for dense two-dimensional specimens close to point at which the peak stress is mobilized.

REFERENCES

Bolton, M.D. (1986) "The strength and dilatancy of *sands" Geotechnique* 36 (1) 65-78.

Gudehus, G. and Nubel, K (2004) "Evolution of shear bands in sand" *Geotechnique* 54(3) 187-201.

Itasca Consulting Group (2002) PFC2D – Particle Flow Code in Two Dimensions.

Oda, M. and Kazama, H. (1998) "Microstructure of shear bands and its relation to the mechanisms of dilatancy and failure of dense granular soils" *Geotechnique* 48(4) 465-481.

O'Sullivan, C. (2002) *The Application of Discrete Element Modelling to Finite Deformation Problems in Geomechanics* PhD thesis, University of California, Berkeley.

O'Sullivan, C., Bray, J.D. and Li, S. (2003) "A new approach for calculating strain for particulate media" International Journal for Numerical and Analytical Methods in Geomech. 27(10), 859-877.

O'Sullivan, C., Bray, J.D. and Riemer, M.F. (2002) "The influence of particle shape and surface friction variability on the macroscopic frictional strength of rod-shaped particulate media" *ASCE Journal of Engineering Mechanics* 128(11),1182-1192.

O'Sullivan, C., Bray, J.D., and Riemer, M.F. (2004) "An examination of the response of regularly packed specimens of spherical particles using physical tests and discrete element simulations." *ASCE Journal of Engineering Mechanics*, Vol. 130 No. 10. pp 1140-1150

Rowe, P.W. (1962) "The stress-dilatancy relation for static equilibrium of an assembly of particles in contact" Proc. Royal Society London, Series A, 269(1339) 500-527.

Thomas, P. (1997) *Discontinuous Deformation Analysis of Particulate Media* PhD thesis, University of California, Berkeley.